applied sciences

MDPI

Article

Fast Neutron and Gamma-Ray Attenuation Properties of Some HMO Tellurite-Tungstate-Antimonate Glasses: Impact of Sm^{3+} Ions

Ghada ALMisned [1], Huseyin O. Tekin [2,3,*], Hesham M. H. Zakaly [4,5,*], Shams A. M. Issa [4,6], Gokhan Kilic [7], Heba A. Saudi [8], Merfat Algethami [9] and Antoaneta Ene [10,*]

1 Department of Physics, College of Science, Princess Nourah Bint Abdulrahman University, Riyadh 11671, Saudi Arabia; gaalmisned@pnu.edu.sa
2 Medical Diagnostic Imaging Department, College of Health Sciences, University of Sharjah, Sharjah 27272, United Arab Emirates
3 Medical Radiation Research Center (USMERA), Uskudar University, Istanbul 34672, Turkey
4 Physics Department, Faculty of Science, Al-Azhar University, Assiut 71524, Egypt; sh_issa@ut.edu.sa
5 Institute of Physics and Technology, Ural Federal University Yekaterinburg, 620002 Yekaterinburg, Russia
6 Physics Department, Faculty of Science, University of Tabuk, Tabuk 71491, Saudi Arabia
7 Department of Physics, Faculty of Science and Letters, Eskisehir Osmangazi University, Eskisehir 26040, Turkey; gkilic@ogu.edu.tr
8 Physics Department, Faculty of Science (Girls Branch), Al-Azhar University, Nasr City 11884, Egypt; heba_saudi@azhar.edu.eg
9 Physics Department, Faculty of Science, Taif University, Taif 21944, Saudi Arabia; M.algethami@tu.edu.sa
10 INPOLDE Research Center, Department of Chemistry, Physics and Environment, Faculty of Sciences and Environment, Dunarea de Jos University of Galati, 800008 Galati, Romania
* Correspondence: htekin@sharjah.ac.ae (H.O.T.); h.m.zakaly@gmail.com (H.M.H.Z.); Antoaneta.Ene@ugal.ro (A.E.)

check for updates

Citation: ALMisned, G.; Tekin, H.O.; Zakaly, H.M.H.; Issa, S.A.M.; Kilic, G.; Saudi, H.A.; Algethami, M.; Ene, A. Fast Neutron and Gamma-Ray Attenuation Properties of Some HMO Tellurite-Tungstate-Antimonate Glasses: Impact of Sm^{3+} Ions. *Appl. Sci.* **2021**, *11*, 10168. https://doi.org/10.3390/app112110168

Academic Editor: Luigi Biolzi

Received: 13 September 2021
Accepted: 26 October 2021
Published: 29 October 2021

Publisher's Note: MDPI stays neutral with regard to jurisdictional claims in published maps and institutional affiliations.

Copyright: © 2021 by the authors. Licensee MDPI, Basel, Switzerland. This article is an open access article distributed under the terms and conditions of the Creative Commons Attribution (CC BY) license (https://creativecommons.org/licenses/by/4.0/).

Abstract: Characteristics of tellurite-tungstate-antimonate glasses containing heavy metal oxide were investigated in detail using two methods: the MCNPX Monte Carlo code and the Phy-X/PSD platform. The influence of Sm_2O_3, translocating with TeO_2 at ratios of 0.2, 0.5, 0.8, 1, and 1.5 mol% on radiation shielding properties of glasses, was set forth with five glass structures determined according to the (75-x)TeO_2-15Sb_2O_3-10WO_3-xSm_2O_3 glass composition. Densities of the glasses were prepared by doping a low ratio of Sm_2O_3 that varied between 5.834 and 5.898 g/cm^3. Sample densities, which have an important role in determining radiation shielding character, increased depending on the increase in Sm_2O_3 concentration. Effective removal cross-section (∑R) values against fast neutrons, as well as linear and mass attenuation coefficients, half-value layer, mean free path, variation of effective atomic number against photon energy, exposure, and energy built-up factors, were simulated with the help of these two methods. As a result of these estimates, it can be concluded that values obtained using both methods are consistent with each other. From the obtained values, it can be concluded that the SM1.5 sample containing 1.5 mol% would have the most efficient role in radiation shielding. An increase of Sm_2O_3 resulted in a significant increase in linear and mass attenuation coefficients and effective removal cross-section values belonging to fast neutrons and, in addition, resulted in a decrease in the half value layer. Doping HMO glasses with Sm_2O_3 was observed to contribute directly to the development of radiation shielding properties of the glass.

Keywords: heavy metal oxide glasses; fast neutron; gamma-ray; MCNPX; Phy-X/PSD; samarium

1. Introduction

Among the many kinds of glasses, heavy metal oxide (HMO) glasses have garnered considerable attention recently due to their low-phonon properties [1,2]. Heavy metal oxide glasses comprise more than 50% mol percent of a HM cation.

On the other hand, TeO_2, Sb_2O_3, Bi_2O_3, and PbO are all known representatives of the HMO glass family. These glasses are superior photonic matrices due to their wider transparency interval spanning the visible to the mid-infrared range, improved non-linear optical features, the high solubility of rare-earth ions, and lower phonon energies than phosphate borate glasses and silicate glasses. Besides their outstanding thermal, mechanical, and chemical resistance, heavy metal oxide glasses have exceptional optical and electrical properties, including a high refractive index and dielectric constant. Therefore, heavy metal oxide glasses are good prospects for a variety of optoelectronic applications, including fiber optics, lasers, and sensors. However, material density (g/cm^3) is a basic necessity of potential substances for gamma radiation shielding applications. On the other hand, tellurium dioxide (TeO_2) is incapable of forming a glassy network under normal quenching conditions without the aid of a secondary material component known as a network modifier. Due to this characteristic, TeO_2 is a conditional glass former [3,4]. A study of the literature revealed that HMO glasses had been examined for their gamma ray attenuation characteristics, which are a result of their high material density. Celikbilek Ersundu et al., conducted several investigations on manufactured HMO glasses with nominal compositions of K_2O–WO_3–TeO_2 and ZnO–MoO_3–TeO_2 [5,6]. As per their results, K30W60T10 and Z10M10T80 glasses were found to be the most efficient shielding glasses due to their increased resistance to ionizing gamma rays. Our research established that these two glass samples are comparable as they had the highest TeO_2 ratio in their structure.

Additionally, a review of the literature showed that a substantial amount of research had been conducted on HMO-Reinforced glasses. Al-Hadeethi and Sayyed, for example, used the Geant4 simulation code to analyze particular HMO doped borosilicate glasses [7]. Their results indicated that the addition of three dopants, namely Bi_2O_3, BaO, and TiO_2, caused a reduction in the HVL, thus improving the attenuation performance of the investigated HMO glasses. D'Souza et al. examined the impact of Bi_2O_3 on the structural, optical, mechanical, radiation shielding, and luminescence properties of borosilicate glasses containing HMO in another research [8]. Their findings showed that although the gamma-ray shielding capacity increased with successive applications of Bi_2O_3, the neutron attenuation capacity decreased. Our previous studies have led us to further studies on HMO glasses that integrate more extensive concepts. In this study, some of the promising and highly dense Sm_2O_3 reinforced HMO glasses [9] have been selected from the literature. Accordingly, some of the significant contributions of Sm_2O_3 additive to the fast neutron and gamma-ray attenuation characteristics of HMO glasses were studied using mathematical and simulation approaches. The results of radiation shielding properties are determined using MCNPX Monte Carlo code and Phy-X/PSD and then discussed considering the Sm_2O_3 additive in each glass sample. We hypothesized that TeO_2/Sm_2O_3 substitution could change the gamma-ray and fast neutron properties of the HMO glasses. Therefore, each finding of the investigation will be addressed to the given scientific hypothesis. Considering the importance of HMO glasses in the literature and their shielding applications in various radiation facilities, the current study's findings may offer some promising and valuable insights into the existing HMO glass and radiation shielding literature.

2. Materials and Methods

A group of heavy metal oxide glasses based on the nominal composition of (75-x)TeO_2-15Sb_2O_3-10WO_3-xSm_2O_3 (where; x = 0.2, 0.5, 0.8, 1, and 1.5 mol%) have been selected from the literature [9], where the authors have performed a characterization study on those glasses in terms of their luminescence properties. Their research findings encouraged us to broaden the scope of the characterization by including certain critical glass characteristics, namely nuclear radiation shielding capabilities. The compositions of the studied glass samples can be listed as follows.

- 74.8TeO_2-15Sb_2O_3-10WO_3-0.2Sm_2O_3
- 74.5TeO_2-15Sb_2O_3-10WO_3-0.5Sm_2O_3
- 74.2TeO_2-15Sb_2O_3-10WO_3-0.8Sm_2O_3

- $74TeO_2$-$15Sb_2O_3$-$10WO_3$-$1Sm_2O_3$
- $73.5TeO_2$-$15Sb_2O_3$-$10WO_3$-$1.5Sm_2O_3$

Accordingly, we used two different tools to determine the critical gamma-ray shielding properties along with some mathematical applications for determining the effective removal cross section (∑R) values for fast neutrons. The linear attenuation coefficients of the glasses were derived using the general-purpose Monte Carlo software MCNPX (v.2.7.0) [10] and the online computation platform Phy-X/PSD [11]. The purpose of this dual tool method was to assess the consistency of the findings obtained from Monte Carlo simulations.

2.1. Technical Information of MCNPX Simulations

MCNPX is a general-purpose Monte Carlo code that can be used in different types of radiation transport simulations in nuclear, medical, and particle physics studies. This code enables the user to provide the simulation's necessary characteristics, including geometrical details, material properties, and the radiation source's energy and type, such as narrow beam, point isotropic, and so on. Our study defined a general gamma-ray transmission setup, which can provide basic information, such as the intensity of attenuated gamma-ray in terms of determining the linear attenuation coefficients. We developed a fundamental gamma-ray transmission setup in our research that may give fundamental information, such as the intensity of the attenuated gamma-ray when calculating the linear attenuation coefficients. Accordingly, an INPUT file was created considering cell card, surface card, and source information [10]. In the cell card, we identified the cells that were utilized and their densities and borders. Geometrical features of the boundaries have been specified in the surface card using the x, y, and z axis positions. Figure 1 depicts the modelled simulation setup along with its 3-D and 2-D views obtained from MCNPX visual editor. As it is seen from Figure 1, we set the locations of the used equipment considering their roles for gamma-ray transmission simulation. For instance, a gamma-ray attenuator has been placed between the source of point-isotropic radiation and the detecting field (F4 Tally Mesh). Additionally, two large Lead (Pb) blocks have been designed to absorb scattering gamma-rays, which may increase detection consistency. We would like to emphasize that simulations were performed on each glass sample using photon energy ranging from 0.015 MeV to 15 MeV. Finally, it is worth noting that each glass sample received a total of 10^8 particle tracks (Number of History) with various photon energies. After running all simulations, the MCNPX output exhibited a relative error rate of less than 1%. MCNPX simulations were performed in Lenovo™ ThinkStation620, which has a Ryzen™ Threadripper™ Pro 3995WX (2.7 GHz, 64 Cores, 256 MB Cache) processor. Next, a Phy-X/PSD platform was used to determine the attenuation coefficients. The main difference between the MCNPX and Phy-X/PSD is their format. On the one hand, MCNPX is a Monte Carlo algorithm that needs user definitions for almost every element of the system, including material design, simulation environment, physics list used, and variance reduction methods. On the other hand, Phy-X/PSD is a platform that delivers results immediately as a consequence of mathematical computations performed against a predefined database. Additional information may be acquired from the original article, which is available elsewhere [11].

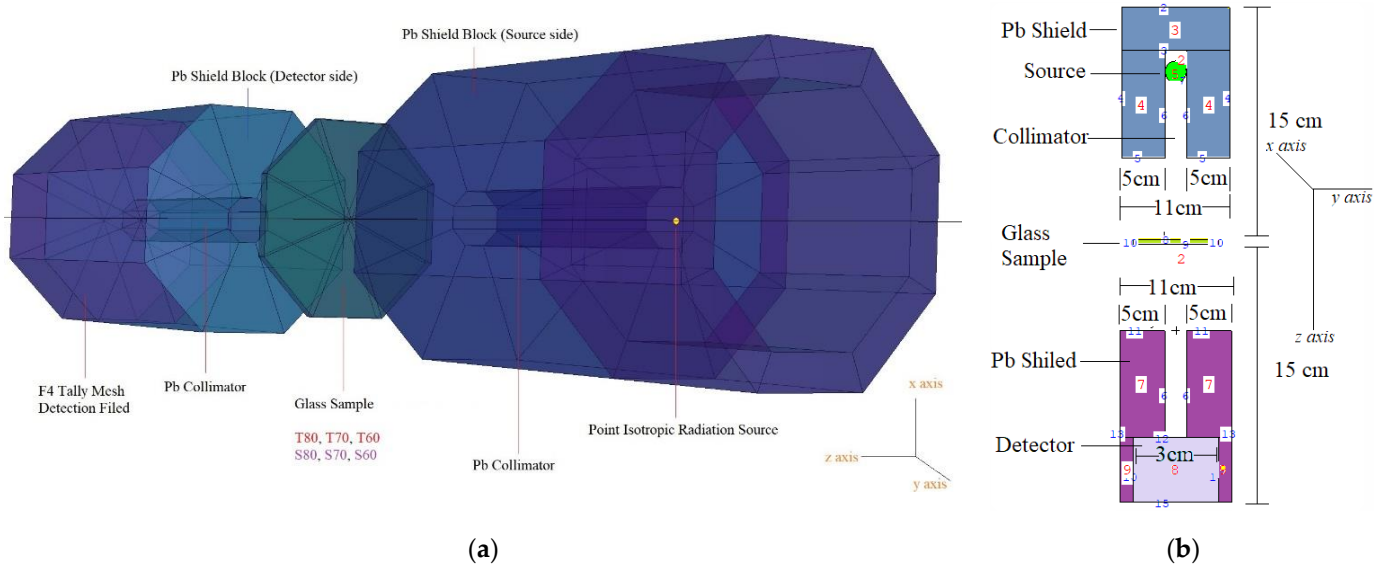

(**a**) (**b**)

Figure 1. MCNPX simulation setup used for gamma-ray transmission simulations (**a**) direct screenshot from the MCNPX Visual Editor VE X_22S. (**b**) 2D view of simulation setup obtained from MCNPX visual editor.

2.2. Studied Nuclear Radiation Shielding Parameters

Several additional gamma radiation attenuation parameters were calculated after finding the linear attenuation coefficients (μ). To begin, we used Equation (1) to calculate the mass attenuation coefficients (μ_m) of the SM glasses [12].

$$\mu_m = \frac{\mu}{\rho} \tag{1}$$

where μ is the linear attenuation coefficient, and ρ is the glass density. Following that, the SM glasses' half value layer ($T_{1/2}$) values were calculated. $T_{1/2}$ is a key factor in determining the need for very stringent radiation protective measures [13]. This quantity provides remarkable information about the thickness of a shielding material at which the intensity of a gamma ray received on it is effectively halved. Additionally, key gamma ray shielding characteristics, such as mean free path (λ) [14], effective atomic numbers (Z_{eff}) [15] against gamma-ray attenuation, exposure, and energy absorption build-up factors (EBF and EABF) [16–20], were measured throughout the gamma-radiation energy range of 0.015–15 MeV. On the other side, we aimed to evaluate the SM glasses' attenuation properties against fast neutrons, which can be beneficial for special utilizations in neutron used/expected (i.e., photodisintegration) radiation facilities. As a result, we calculated the effective removal cross-sections of SM glasses against fast neutrons (∑R) [21,22]. Detailed information on the parameters under investigation may be found in the literature and elsewhere [23–25].

3. Results and Discussion

In this study, five different Sm_2O_3-reinforced heavy metal oxide glasses based on the nominal composition of (75-x)TeO_2-15Sb_2O_3-10WO_3-xSm_2O_3 (where; x = 0.2, 0.5, 0.8, 1, and 1.5 mol%) have been investigated in terms of their gamma-ray and neutron shielding properties. First, we calculated the linear attenuation coefficients by using MCNPX code. Following the given details above, linear attenuation coefficients for each glass sample were determined at different energies that varied from 0.015 MeV to 15 MeV. Next, the same glass compositions (see Table 1) along with their densities were defined in the Phy-X/PSD platform. Overall, the obtained results agreed well with each other.

Table 1. Chemical compositions (mol%) and density values of HMO glasses.

Sample Code	TeO_2	Sb_2O_3	WO_3	Sm_2O_3	Density (g/cm^3)
SM0.2	74.8	15	10	0.2	5.834
SM0.5	74.5	15	10	0.5	5.841
SM0.8	74.2	15	10	0.8	5.852
SM1.0	74	15	10	1	5.865
SM1.5	73.5	15	10	1.5	5.898

Figure 2 shows the comparison of obtained μ values from MCNPX and Phy-X/PSD at low energy region (i.e., 0.015 MeV, 0.02 MeV, 0.03 MeV, 0.04 MeV, 0.05 MeV, 0.06 MeV, and 0.0 MeV). As shown in Figure 2, there is a strong correlation between the two results. However, we discovered some minor inconsistencies as well. Due to the fact that the MCNPX and Phy-X/PSD formats are diametrically opposed, it is quite reasonable to anticipate some discrepancies in the results. MCNPX is a user-friendly program that needs certain fundamental processes, such as material design and source specification.

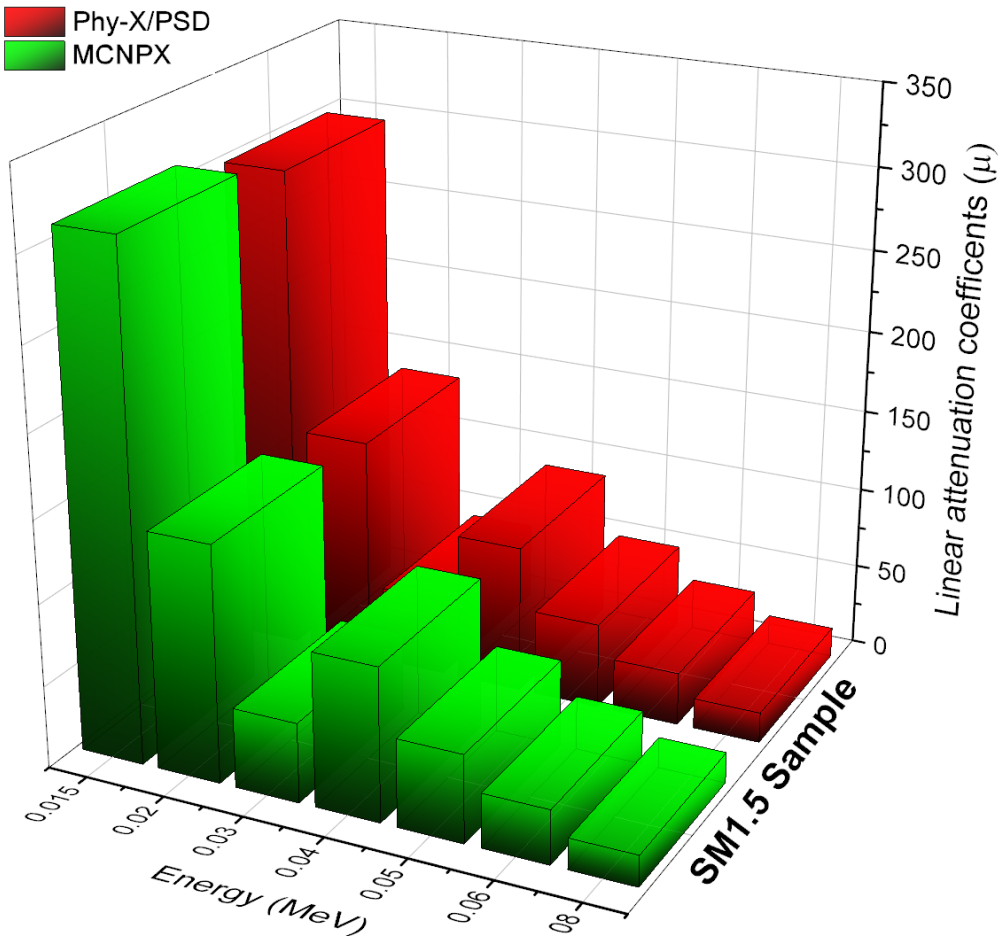

Figure 2. Comparison of linear attenuation coefficient (μ) values for SM1.5 sample obtained from MCNPX and Phy-X/PSD at low gamma ray energy region.

On the other hand, there is a direct correlation between a computer's performance and its relative error. Additionally, there are many sub-titles that may affect the consistency of the Monte Carlo simulation results. However, Phy-X/PSD is a web-based platform that enables users to get different shielding characteristics based on just the material description and energy range. It is worth noting that the total relative variation between the findings ranged from 1.2% to 2.9%. After checking the consistency of the tools, we proceed to the following parameters. Meanwhile, our results indicate that the SM1.5 sample exhibits

the highest linear attenuation coefficients throughout the whole energy range. This may be explained partly by the glass densities, as well as the chemical compositions listed in Table 1. Figure 3 illustrates the difference in glass densities. As can be observed, density levels significantly increased from SM0.2 to SM1.5. As seen in Table 1, increasing the Sm_2O_3 reinforcements also improved the glass density. Our findings indicated that adding Sm_2O_3 to HMO glasses enhanced their density and, therefore, their linear attenuation coefficients.

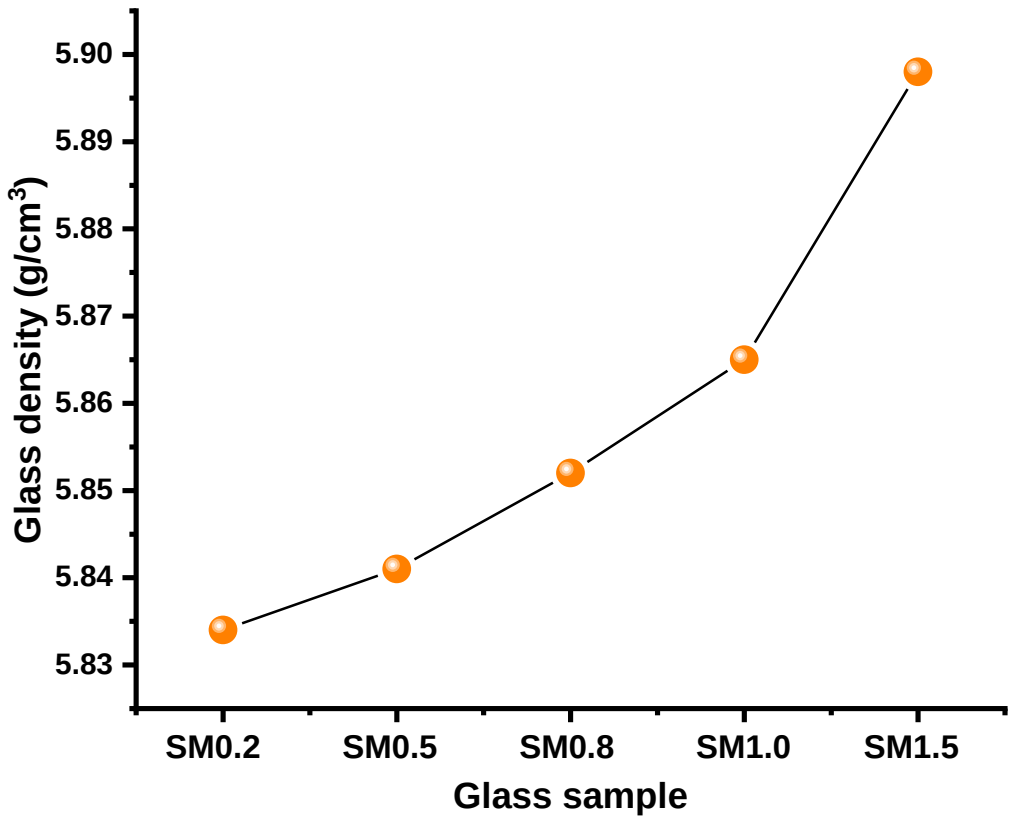

Figure 3. Variation of glass densities as a function of glass type (i.e., Sm_2O_3 %mol).

At this moment, Figure 4 depicts the changes in μ values as photon energy (MeV) function. From 0.015 MeV to 0.03 MeV, a sharp decrease was seen. Following that, a sharp peak near Te's k-absorption edge was found. This demonstrates that Te is present in all glass samples. We would like to emphasize that the results of the glass samples were near to each other due to the low molar variations in the Sm_2O_3 additive. Nevertheless, adding the Sm_2O_3 additive had a synergistic impact on the linear attenuation coefficients of SM glasses. Our findings clearly showed that the SM1.5 sample has the maximum μ values at all energies. On the other hand, the term mass attenuation coefficient (μ_m) refers to the density-independent attenuation coefficient, which contains critical information about the material's shielding performance as a function of its elemental structure.

Figure 5 illustrates the variation of μ_m values in the low-energy region. Similar to the discovery of μ values, the SM1.5 sample was reported with maximum amounts. This is explained by the fact that replaced TeO_2 and Sm_2O_3 have different elemental structures and atomic numbers, directly affecting gamma-ray attenuation properties.

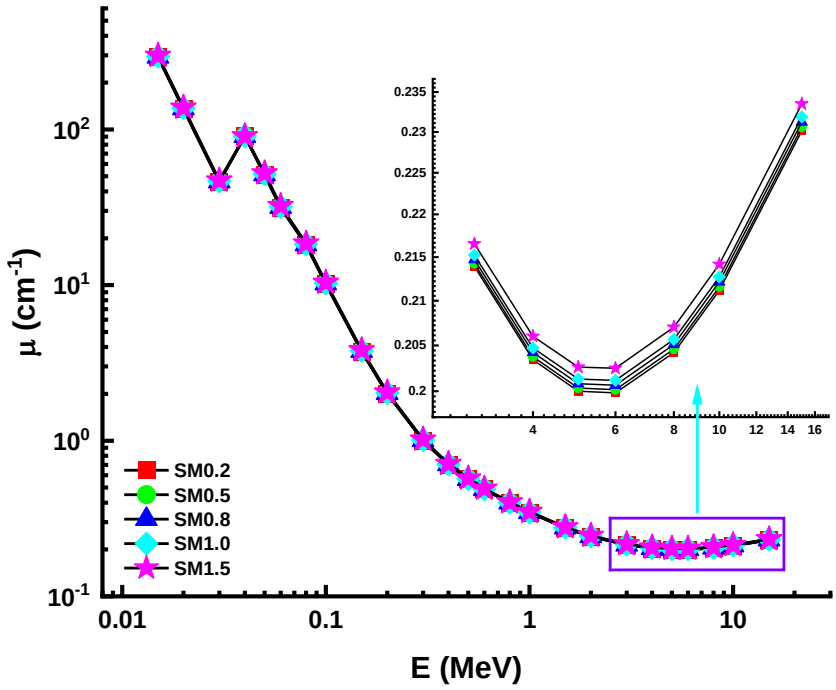

Figure 4. Variation of linear attenuation coefficient (μ) against Photon energy for all glasses.

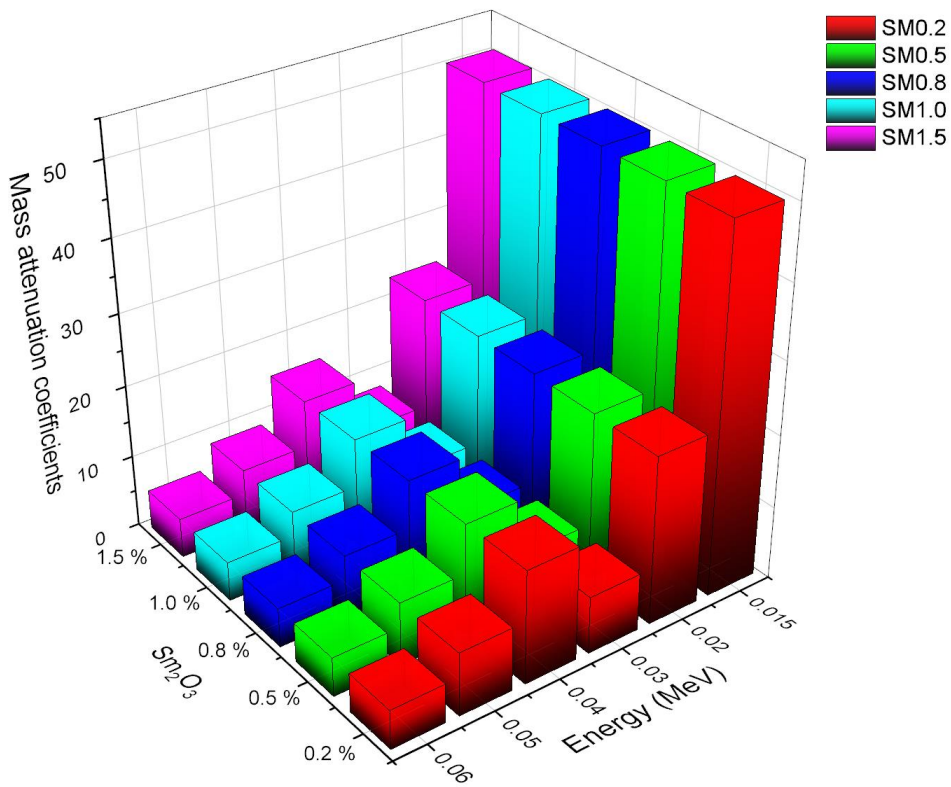

Figure 5. Variation of mass attenuation coefficients (μ_m) at low energy region.

Meanwhile, Figure 5 clearly demonstrated the Te k-absorption peak, indicating that the overwhelming majority of the nominal glass composition was TeO_2. In addition, we demonstrated the variation of μ_m values as a function of photon energy from 0.015 MeV to 15 MeV. The dominance of main photon–matter interactions, such as photoelectric effect, Compton scattering, and pair production, can be observed in Figure 6.

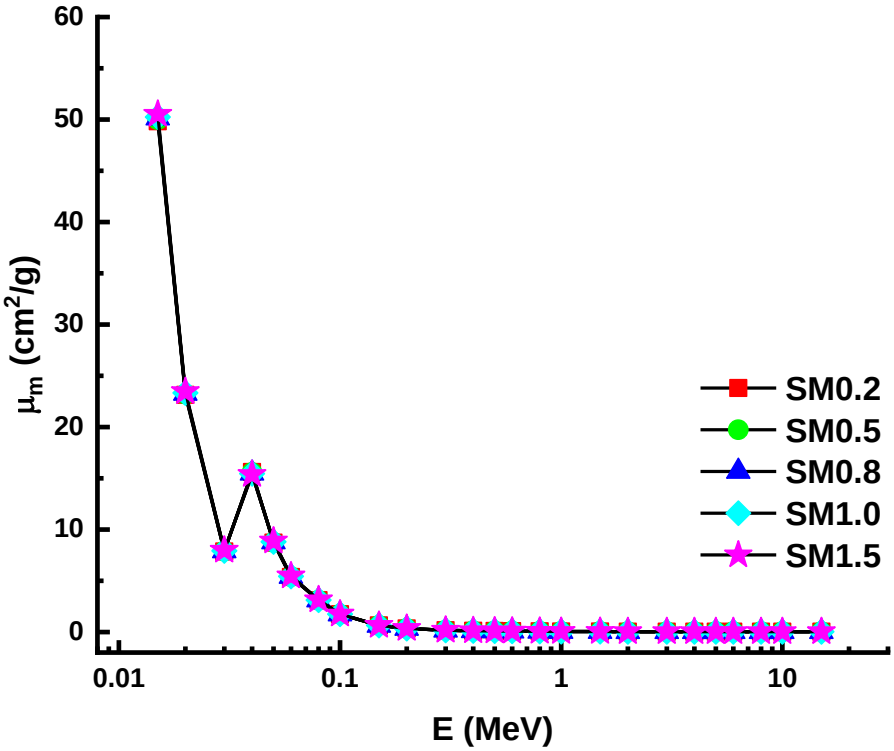

Figure 6. Variation of mass attenuation coefficient (μ_m) against Photon energy for all glasses.

According to findings, SM1.5 has the maximum μ_m values among the studied SM glass samples. In this study, half value layers ($T_{1/2}$) of SM glasses were also determined between 0.015 MeV and 15 MeV. The term $T_{1/2}$ is crucial for determining the thickness of a shielding material needed to reduce the initial gamma-ray intensity to half Figure 7. It is worth noting that the $T_{1/2}$ term has an inverse relationship with the μ value, which implies that material with higher μ values may also offer lower $T_{1/2}$ values. Additionally, a material with the lowest $T_{1/2}$ values may be regarded as a clear indicator of gamma-ray superiority among the studied material group. Our results indicated that the SM1.5 sample with the highest Sm_2O_3 additive has the lowest $T_{1/2}$ values at all energy levels. For example, $T_{1/2}$ values were reported as 2.00553 cm, 2.00262 cm, 1.99835 cm, 1.99359 cm, and 1.98160 cm for SM0.2, SM0.5, SM0.8, SM1.0, and SM1.5 samples at 1 MeV, respectively. At this moment, it can be noted that 1.3% mol Sm_2O_3 (i.e., from 0.2% to 1.5%) decreased the $T_{1/2}$ value from 2.00553 cm to 1.98160 cm.

As with pure elements, the atomic numbers of compounds, alloys, and composite materials cannot be represented by a single number in the various energy zones. This number is referred to as the effective atomic number (Z_{eff}) for compounds, alloys, and mixtures, and it changes according to the photon energy [26]. Figure 8 depicts the variation of Z_{eff} as a function of incident photon energy at all energies. The results indicated that the sample with the highest Zeff value is SM1.5, with the most Sm_2O_3 in the structure. However, no sharp differences were reported due to the structural similarities between the samples. It should be noted that the minimum difference for Z_{eff} values was reported as 0.07 at 0.04 MeV, whereas the maximum difference was 0.36 at 0.06 MeV.

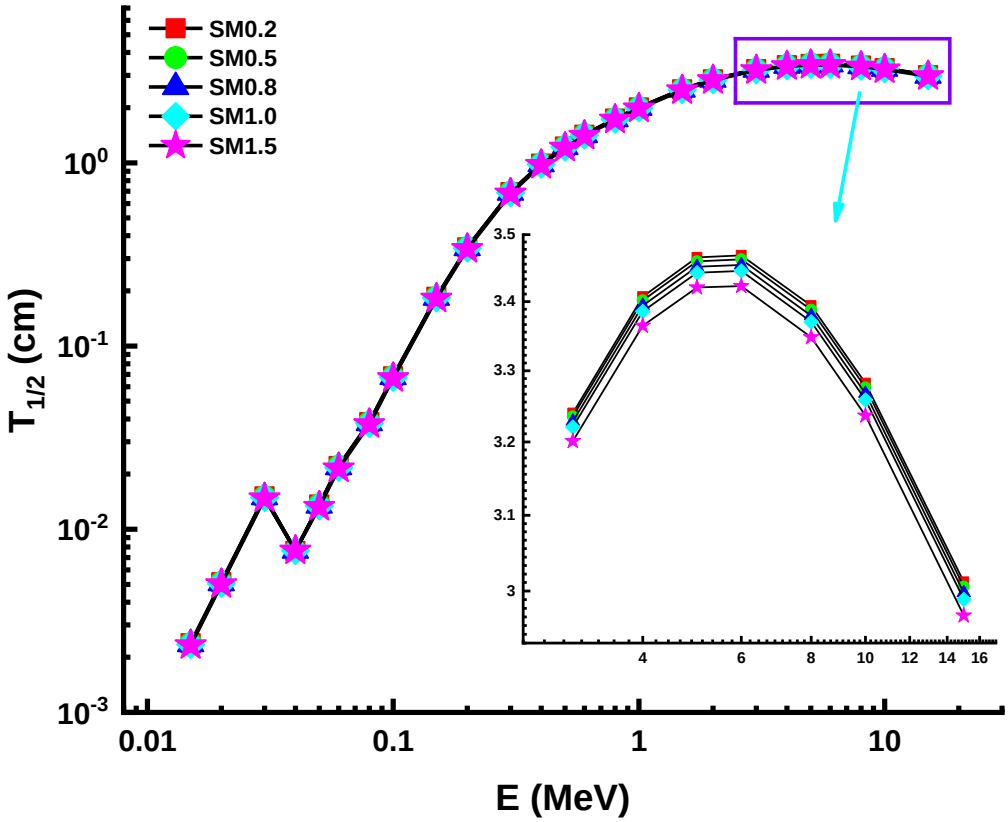

Figure 7. Variation of half value layer ($T_{1/2}$) against Photon energy for all glasses.

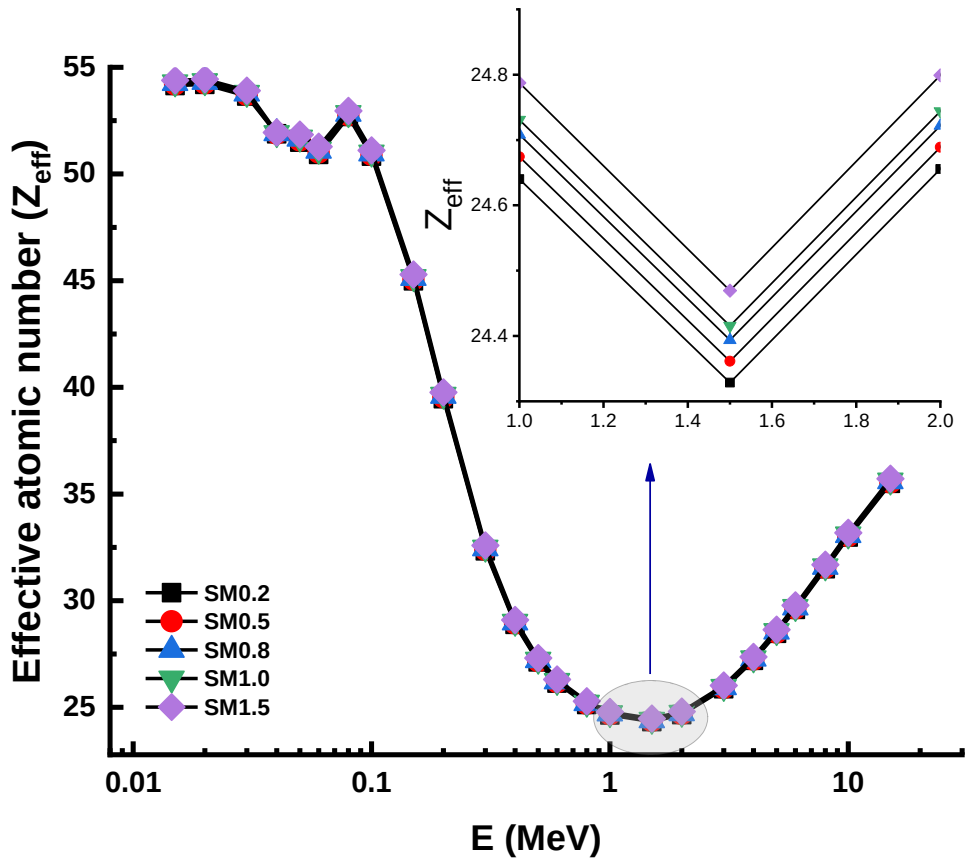

Figure 8. Variation of effective atomic number (Z_{eff}) against Photon energy for all glasses.

The buildup factor is a correction factor used in shielding computations to account for the effect of scattered radiation and any secondary particles in the medium. If one intends to compensate for secondary radiation accumulation, one must add a buildup factor. The accumulation factor is thus a multiplicative factor that incorporates the contribution of the scattered photons into the reaction to the uncollided photons. Thus, the accumulation factor may be calculated as the ratio of the entire dosage to the uncollided dose-response [27]. Meanwhile, the term of buildup factor can be classified as to exposure buildup factor (EBF) and energy absorption buildup factor (EABF) [28]. In parallel to the given description, the lower buildup factor values can be considered a superiority pattern against gamma-rays since the uncollided photon amount in the successful shields would be low. Figures 9 and 10 depicts the variations of EBF and EABF values as a function of energy at various mean free paths (i.e., from 0.5 to 40). The highest values were seen in both EBF and EABF in the mid-energy range, where Compton scattering is the main interaction between the gamma-ray and the material (see Tables S1–S5). In other words, this area has a high amount of uncollided photons. As a result, relatively higher values for the buildup factor are required to correct the transmission calculations. Our results indicate that SM1.5 has the lowest accumulation factors in both EBF and EABF. Thus, incoming gamma-rays may interact with the SM1.5 sample more often than with other samples.

The effective removal cross-section, R (cm^2/g), refers to the possibility that a fast or fission energy neutron would undergo the first collision, thus excluding it from the group of penetrating, uncollided neutrons. For neutron energies between 2 and 12 MeV, it is believed to be roughly constant. Moreover, the materials with the highest ∑R values can be considered as superior materaials against hazardous neutron particles. In this study, ∑R values of SM glasses were determined, and the results have been demonstrated in Figure 11. Following the gamma-ray attenuation characteristics, a distinguished synergistic impact of increasing Sm_2O_3 was eventually found. As shown in Figure 11, the SM1.5 sample clearly differs from the SM0.2 sample. Therefore, one can say that Sm_2O_3 can be considered a useful tool to improve the gamma-ray and fast neutron shielding properties of HMO glasses.

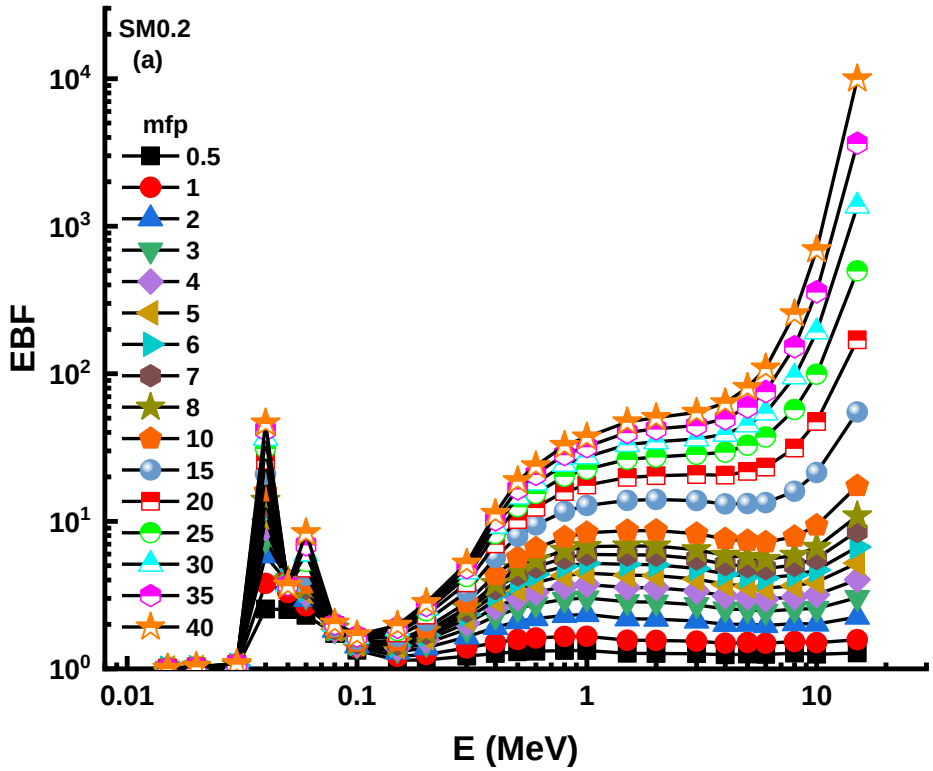

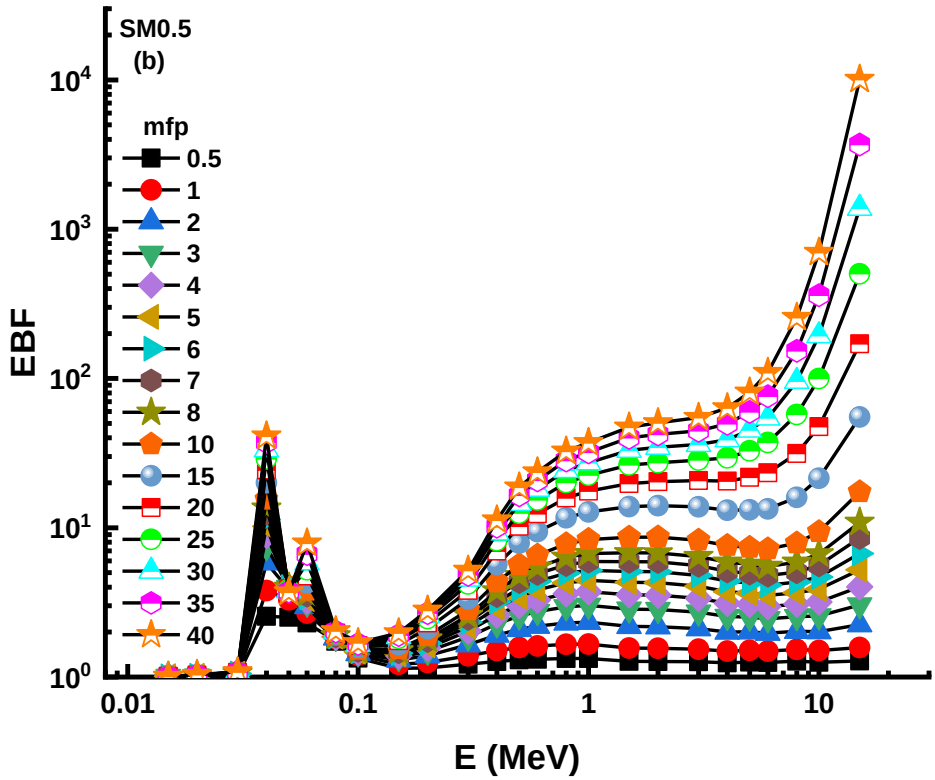

Figure 9. *Cont.*

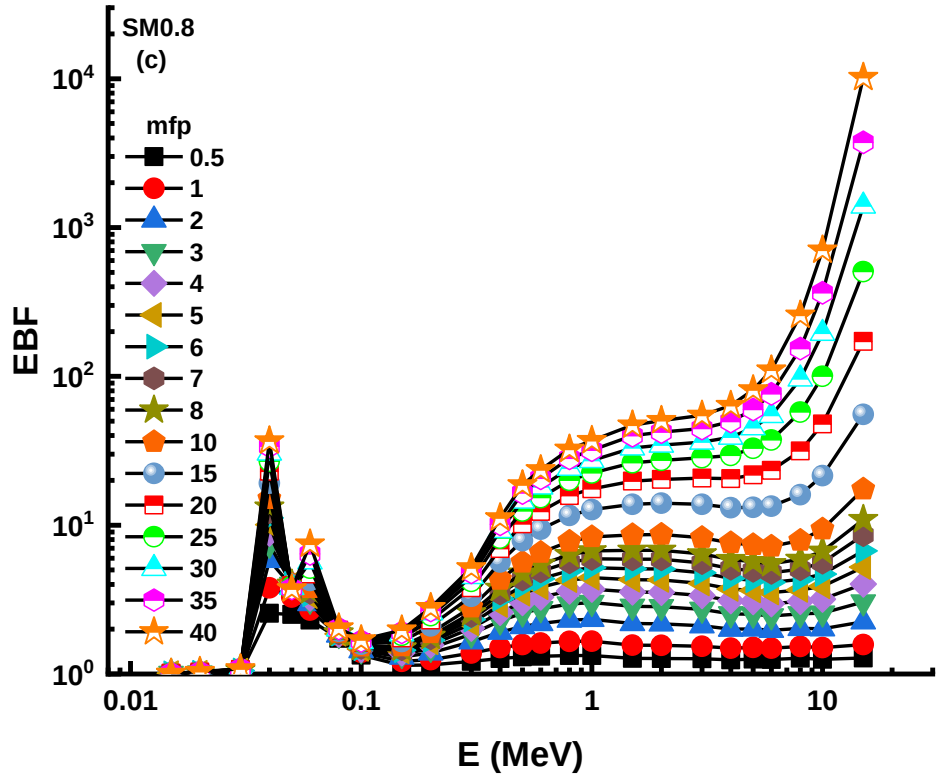

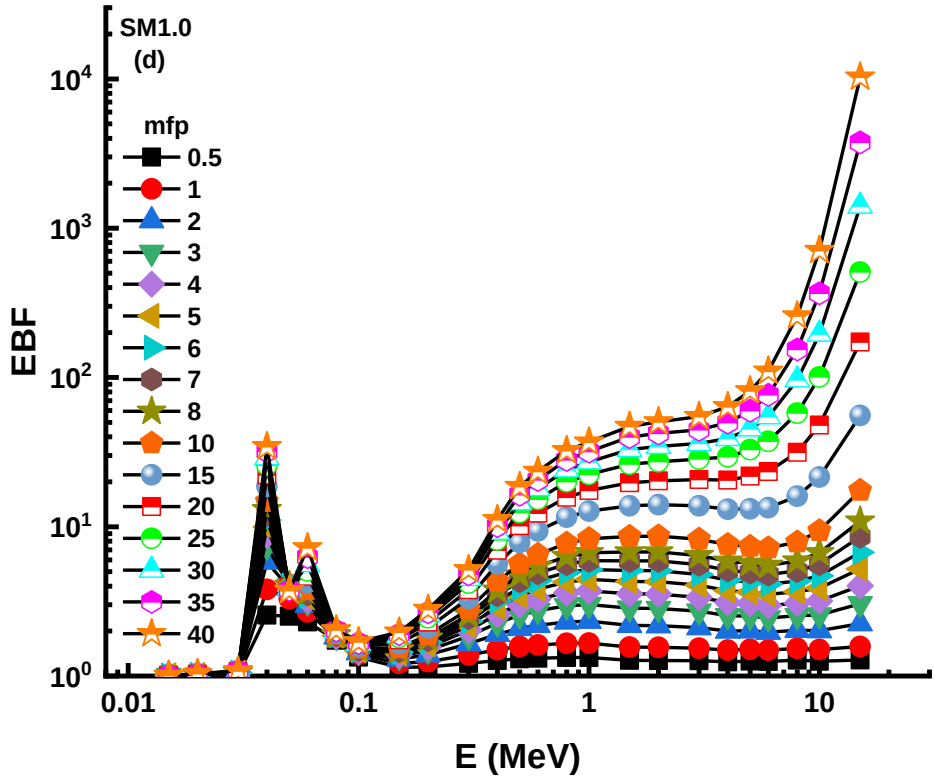

Figure 9. *Cont.*

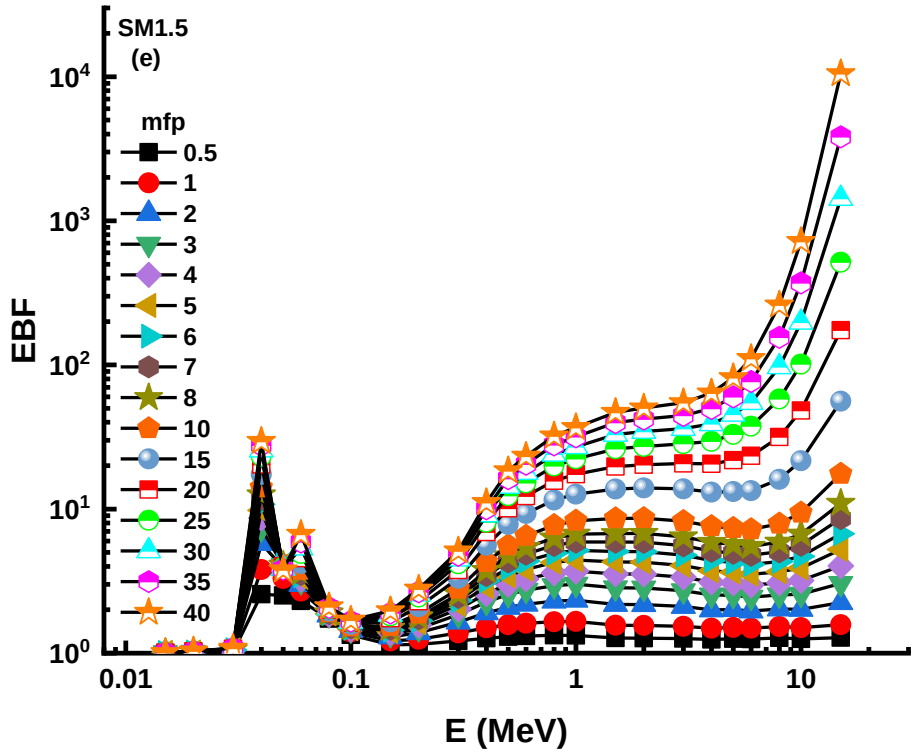

Figure 9. (**a**–**e**). Variation of exposure buildup factor (EBF) against Photon energy for all glasses.

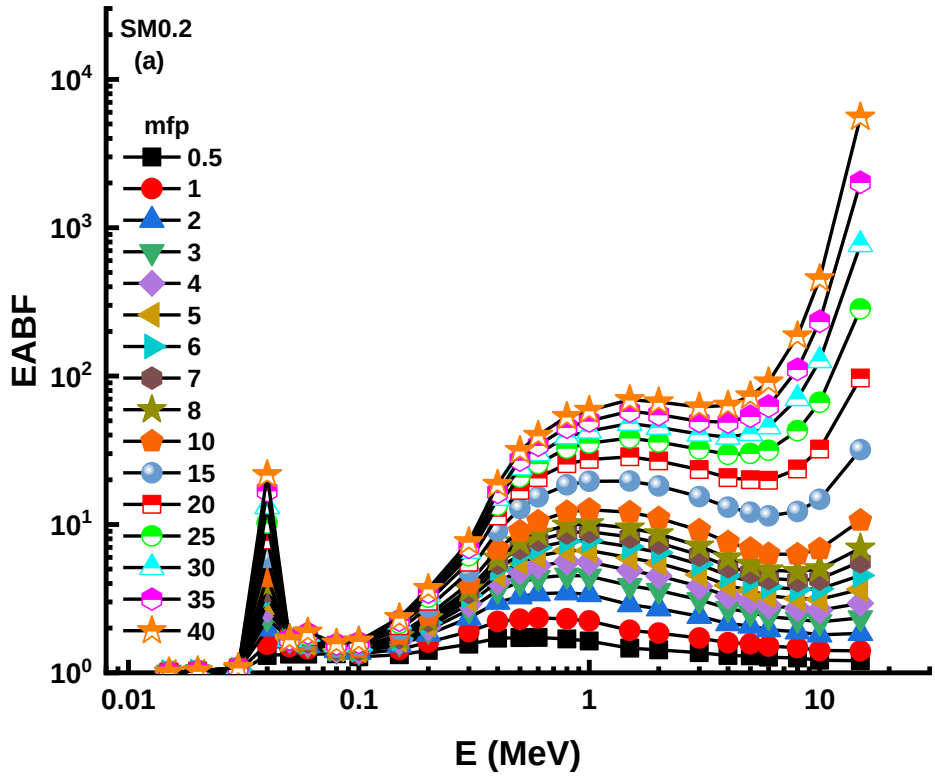

Figure 10. *Cont.*

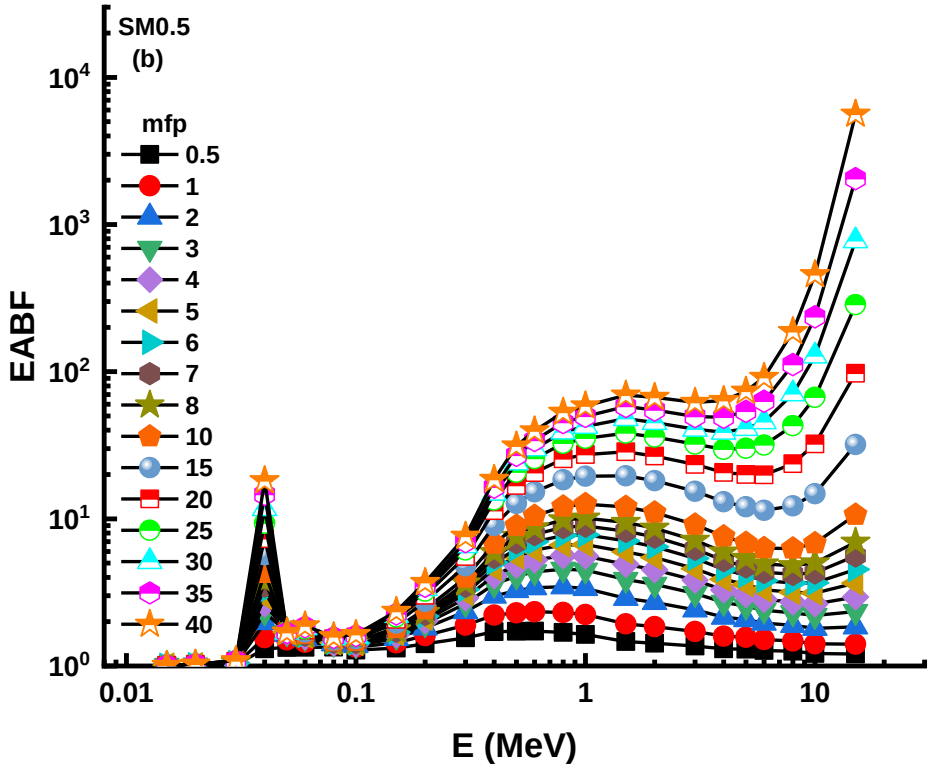

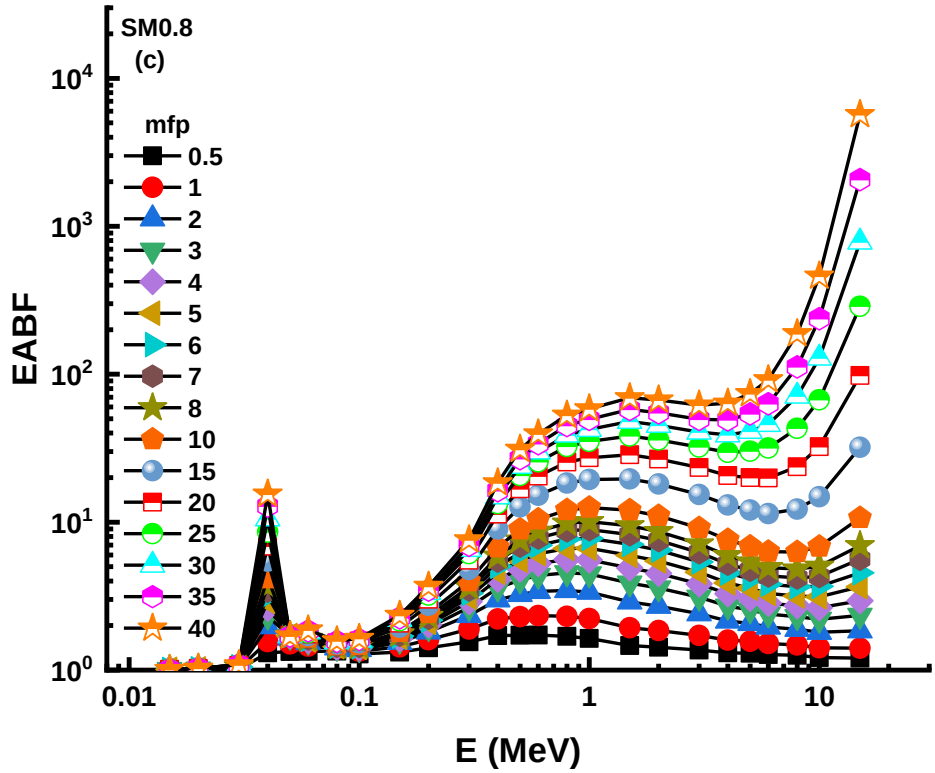

Figure 10. *Cont.*

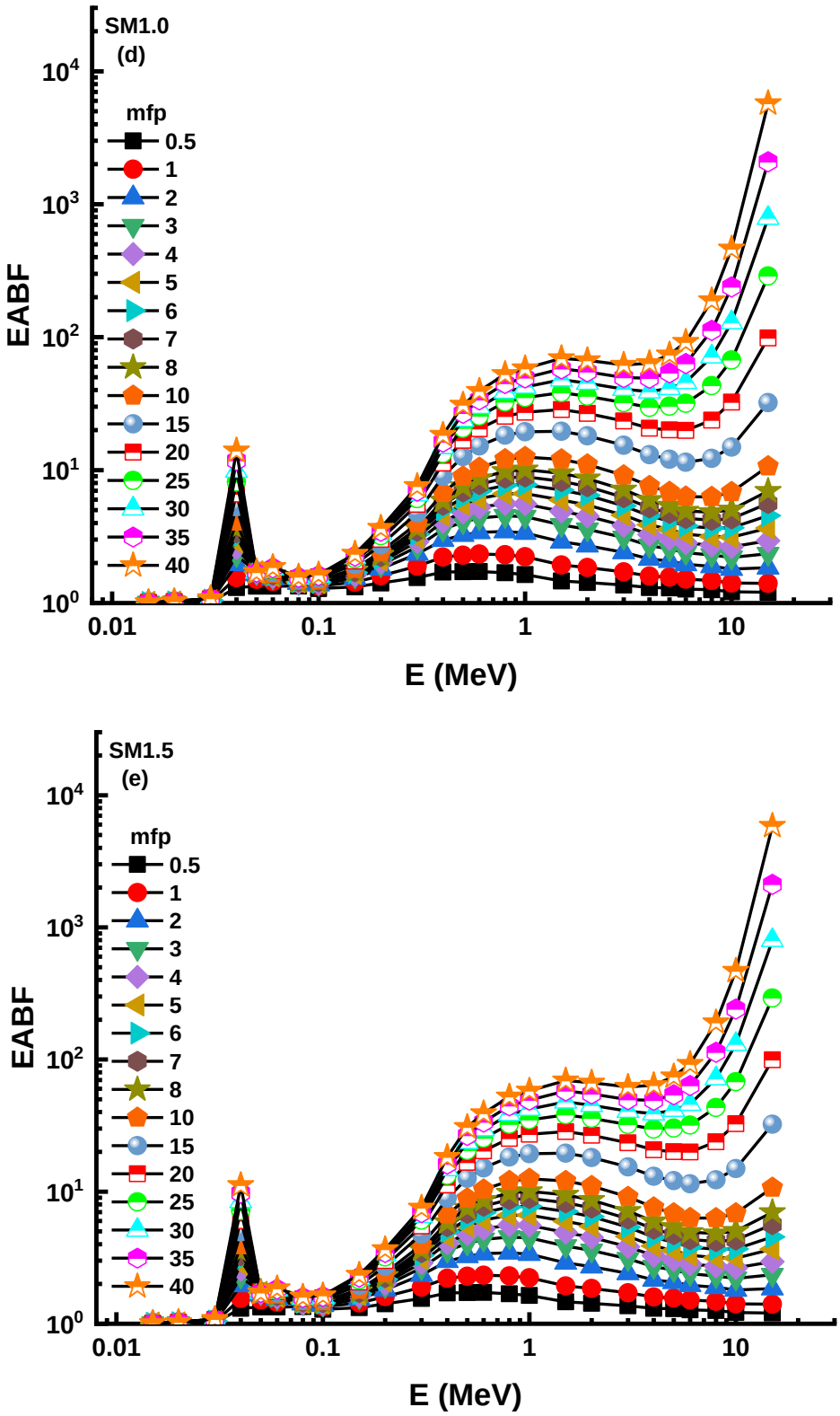

Figure 10. (**a**–**e**). Variation of energy absorption buildup factor (EABF) against Photon energy for all glasses.

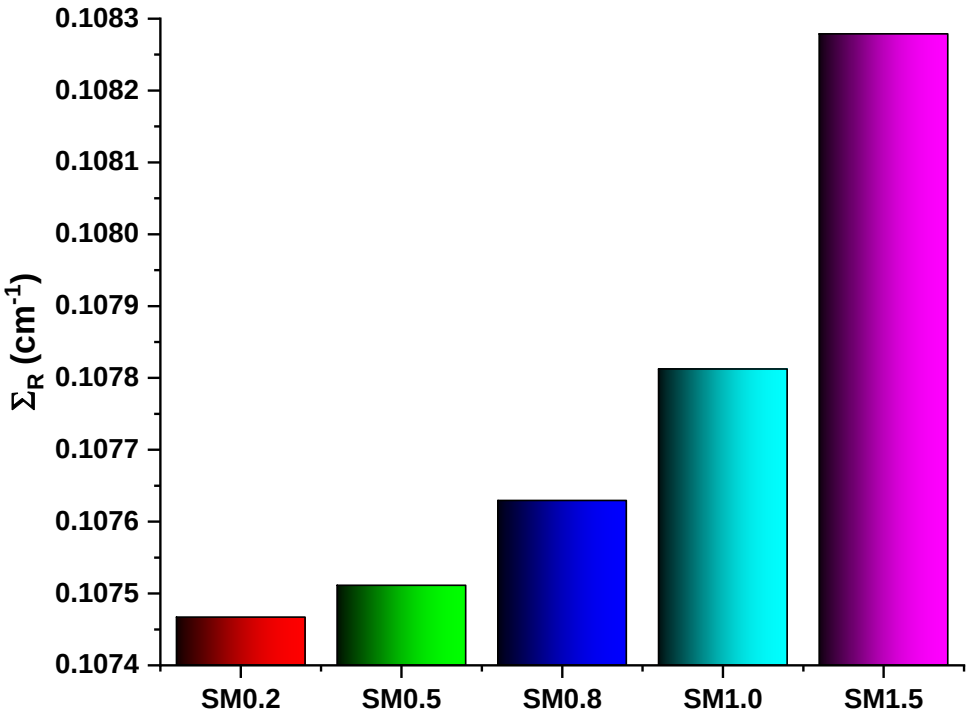

Figure 11. Effective removal cross-sections for fast neutrons (Σ_R) for all glasses.

4. Conclusions

In the current study, we have focused on the radiation shielding characteristics of doped oxide glasses Sm_2O_3 containing a heavy metal oxide. It can be concluded that the inclusion of Sm_2O_3 in heavy metal oxide glasses can be a useful option for improving the capabilities of radiation shielding and other properties of materials, such as optical, luminescence, structural, and thermal. In terms of luminescence characteristics, Sm_2O_3, which has occupied a niche in photonics, may be a favorable compound due to its large size and high density. In fact, the doping of Sm_2O_3 significantly increased the density of the synthesized sample. The results indicated that the SM1.5 sample with the highest Sm_2O_3 additive has the highest density and lowest $T_{1/2}$ values at all energy levels. For example, $T_{1/2}$ values were reported as 2.00553 cm, 2.00262 cm, 1.99835 cm, 1.99359 cm, and 1.98160 cm for SM0.2, SM0.5, SM0.8, SM1.0, and SM1.5 samples at 1 MeV, respectively. At this moment, it can be noted that 1.3% mol Sm_2O_3 (i.e., from 0.2% to 1.5%) decreased the $T_{1/2}$ value from 2.00553 cm to 1.98160 cm. Thus, the SM1.5 glass presents as the best sample for blocking gamma radiation in the current investigation.

Supplementary Materials: The following are available online at https://www.mdpi.com/article/10.3390/app112110168/s1, Table S1: (EBF and EABF) G–P fitting coefficients (b, c, a, Xk and d) of SM0.2 glass sample, Table S2: (EBF and EABF) G–P fitting coefficients (b, c, a, Xk and d) of SM0.5 glass sample, Table S3: (EBF and EABF) G–P fitting coefficients (b, c, a, Xk and d) of SM0.8 glass sample, Table S4: (EBF and EABF) G–P fitting coefficients (b, c, a, Xk and d) of SM1.0 glass sample, Table S5: (EBF and EABF) G–P fitting coefficients (b, c, a, Xk and d) of SM1.5 glass sample.

Author Contributions: Conceptualization, G.A., H.O.T., H.M.H.Z. and S.A.M.I.; methodology, H.O.T.; software, H.O.T., H.M.H.Z. and A.E.; validation, S.A.M.I., G.K. and A.E.; formal analysis, H.M.H.Z., S.A.M.I. and A.E.; investigation, M.A., G.A. and H.O.T.; resources, H.O.T. and G.K.; data curation, G.A., S.A.M.I. and A.E.; writing—original draft preparation, H.O.T. and G.K.; writing—review and editing, H.M.H.Z., H.A.S., S.A.M.I., M.A. and A.E.; visualization, G.A., G.K. and M.A.; supervision, H.M.H.Z., H.A.S. and G.K.; project administration, H.A.S., H.O.T. and S.A.M.I.; funding acquisition, A.E. Researcher H.M.H.Z. funded by a scholarship under the Joint (Executive Program between Egypt and Russia). All authors have read and agreed to the published version of the manuscript.

Funding: This research was funded by the Deanship of Scientific Research at Princess Nourah bint Abdulrahman University through the Fast-track Research Funding Program.

Institutional Review Board Statement: Not applicable.

Informed Consent Statement: Not applicable.

Data Availability Statement: Data is contained within the article.

Acknowledgments: This research was funded by the Deanship of Scientific Research at Princess Nourah bint Abdulrahman University through the Fast-track Research Funding Program. The authors express their thanks to "Dunarea de Jos" University of Galati, Romania, for APC support.

Conflicts of Interest: The authors declare no conflict of interest.

References

1. Ramesh, P.; Gangareddy, J.; Sathish, K.N.; Pramod, A.G.; Hegde, V.; Pasha, U.M.; Khan, S.; Annapurna, K.; Sayyed, M.I.; Alhuthali, A.M.; et al. Effect of heavy metal oxides on photoluminescence and spectroscopic attributes of Eu^{3+} activated borate glasses. *Opt. Mater.* **2021**, *114*, 110933. [CrossRef]
2. Alharbi, T.; Mohamed, H.F.; Saddeek, Y.B.; El-Haseib, A.Y.; Shaaban, K.S. Study of the TiO2 effect on the heavy metals oxides borosilicate glasses structure using gamma-ray spectroscopy and positron annihilation technique. *Radiat. Phys. Chem.* **2019**, *164*, 108345. [CrossRef]
3. Mostafa, A.M.A.; Zakaly, H.M.; Al-Ghamdi, S.A.; Issa, S.A.; Al-Zaibani, M.; Ramadan, R.M.; El Agammy, E.F. PbO–Sb_2O_3–B_2O_3–CuO glassy system: Evaluation of optical, gamma and neutron shielding properties. *Mater. Chem. Phys.* **2021**, *258*, 123937. [CrossRef]
4. Çelikbilek, M.; Ersundu, A.E.; Solak, N.; Aydın, S. Investigation on thermal and microstructural characterization of the TeO_2-WO_3 system. *J. Alloys Compd.* **2011**, *509*, 5646–5654. [CrossRef]
5. Ersundu, M.Ç.; Ersundu, A.E.; Sayyed, M.I.; Lakshminarayana, G.; Aydin, S. Evaluation of physical, structural properties and shielding parameters for K_2O–WO_3–TeO_2 glasses for gamma ray shielding applications. *J. Alloys Compd.* **2017**, *714*, 278–286. [CrossRef]
6. Ersundu, M.Ç.; Ersundu, A.E.; Gedikoğlu, N.; Şakar, E.; Büyükyıldız, M.; Kurudirek, M. Physical, mechanical and gamma-ray shielding properties of highly transparent ZnO-MoO3-TeO2 glasses. *J. Non-Cryst. Solids* **2019**, *524*, 119648. [CrossRef]
7. Al-Hadeethi, Y.; Sayyed, M. Analysis of borosilicate glasses doped with heavy metal oxides for gamma radiation shielding application using Geant4 simulation code. *Ceram. Int.* **2019**, *45*, 24858–24864. [CrossRef]
8. D'Souza, A.N.; Prabhu, N.S.; Sharmila, K.; Sayyed, M.I.; Somshekarappa, H.M.; Lakshminarayana, G.; Mandal, S.; Kamath, S.D. Role of Bi2O3 in altering the structural, optical, mechanical, radiation shielding and thermoluminescence properties of heavy metal oxide borosilicate glasses. *J. Non-Cryst. Solids* **2020**, *542*, 120136. [CrossRef]
9. Rao, V.H.; Prasad, P.S.; Babu, M.M.; Rao, P.V.; Santos, L.; Raju, G.N.; Veeraiah, N. Luminescence properties of Sm^{3+} ions doped heavy metal oxide tellurite-tungstate-antimonate glasses. *Ceram. Int.* **2017**, *43*, 16467–16473. [CrossRef]
10. Radiation Safety Information Computational Center. Collection MCNPX User's Manual Version 2.4.0. In *Monte Carlo N-Particle Transport Code System for Multiple and High Energy Applications*; Radiation Safety Information Computational Center: Oak Ridge, TN, USA, 2002.
11. Şakar, E.; Özpolat, Ö.F.; Alım, B.; Sayyed, M.I.; Kurudirek, M. Phy-X/PSD: Development of a user-friendly online software for calculation of parameters relevant to radiation shielding and dosimetry. *Radiat. Phys. Chem.* **2020**, *166*, 108496. [CrossRef]
12. Saudi, H.A.; Issa, S.A.; Elazaka, A.I.; Zakaly, H.M.; Kilic, G.; Tekin, H.O. Exploration of material characteristics of tantalum borosilicate glasses by experimental, simulation, and theoretical methods. *J. Phys. Chem. Solids* **2021**, *159*, 110282. [CrossRef]
13. Lakshminarayana, G.; Kumar, A.; Tekin, H.; Issa, S.A.; Al-Buriahi, M.; Dong, M.; Lee, D.-E.; Yoon, J.; Park, T. Probing of nuclear radiation attenuation and mechanical features for lithium bismuth borate glasses with improving Bi_2O_3 content for B_2O_3+Li_2O amounts. *Results Phys.* **2021**, *25*, 104246. [CrossRef]
14. Mann, K.S. γ-Ray Shielding Behaviors of Some Nuclear Engineering Materials. *Nucl. Eng. Technol.* **2017**, *49*, 792–800. [CrossRef]
15. AlBuriahi, M.; Hegazy, H.; Alresheedi, F.; Olarinoye, I.; Algarni, H.; Tekin, H.; Saudi, H. Effect of CdO addition on photon, electron, and neutron attenuation properties of boro-tellurite glasses. *Ceram. Int.* **2021**, *47*, 5951–5958. [CrossRef]
16. Bursalıoğlu, E.; Balkan, B.; Kavanoz, H.B.; Okutan, M.; Íçelli, O.; Yalçın, Z. Energy Absorption and Exposure Buildup Factors of Essential Amino Acids. *BioMed Res. Int.* **2014**, *2014*, 1–6. [CrossRef]
17. Rafiei, M.M.; Tavakoli-Anbaran, H. Calculation of the exposure buildup factors for x-ray photons with continuous energy spectrum using Monte Carlo code. *J. Radiol. Prot.* **2017**, *38*, 207–217. [CrossRef] [PubMed]
18. Tekin, H.O.; Issa, S.A.; Kilic, G.Ö.K.H.A.N.; Zakaly, H.M.; Badawi, A.; Bilal, G.; Sidek, H.A.A.; Matori, K.A.; Zaid, M.H.M. Cadmium oxide reinforced $46V_2O_5$–$46P_2O_5$–(8-x)B_2O_3–xCdO semiconducting oxide glasses and resistance behaviors against ionizing gamma rays. *J. Mater. Res. Technol.* **2021**, *13*, 2336–2349. [CrossRef]
19. Singh, V.P.; Badiger, N.M. A Comprehensive Study on Gamma-Ray Exposure Build-Up Factors and Fast Neutron Removal Cross Sections of Fly-Ash Bricks. *J. Ceram.* **2013**, *2013*, 1–13. [CrossRef]

20. Kilic, G.; Ilik, E.; Issa, S.A.; Tekin, H.O. Synthesis and structural, optical, physical properties of Gadolinium (III) oxide reinforced TeO_2-B_2O_3-(20-x) Li_2O-xGd_2O_3 glass system. *J. Alloys Compd.* **2021**, *877*, 160302. [CrossRef]
21. Olarinoye, I.O.; El-Agawany, F.I.; El-Adawy, A.; Rammah, Y.S. Mechanical features, alpha particles, photon, proton, and neutron interaction parameters of TeO2–V2O3–MoO3 semiconductor glasses. *Ceram. Int.* **2020**, *46*, 23134–23144. [CrossRef]
22. Saudi, H.A.; Abd-Allah, W.M.; Shaaban, K.S. Investigation of gamma and neutron shielding parameters for borosilicate glasses doped europium oxide for the immobilization of radioactive waste. *J. Mater. Sci. Mater. Electron.* **2020**, *31*, 6963–6976. [CrossRef]
23. Issa, S.A.; Tekin, H.O. The multiple characterization of gamma, neutron and proton shielding performances of xPbO-(99-x)B_2O_3–Sm_2O_3 glass system. *Ceram. Int.* **2019**, *45*, 23561–23571. [CrossRef]
24. Lakshminarayana, G.; Elmahroug, Y.; Kumar, A.; Tekin, H.O.; Rekik, N.; Dong, M.; Lee, D.E.; Yoon, J.; Park, T. Detailed Inspection of γ-Ray, Fast and Thermal Neutrons Shielding Competence of Calcium Oxide or Strontium Oxide Comprising Bismuth Borate Glasses. *Materials* **2021**, *14*, 2265. [CrossRef] [PubMed]
25. Issa, S.A.M.; Tekin, H.O.; Erguzel, T.T.; Susoy, G. Susoy. The effective contribution of PbO on nuclear shielding properties of xPbO-$(100-x)P_2O_5$ glass system: A broad range investigation. *Appl. Phys. A* **2019**, *125*, 640. [CrossRef]
26. Un, A.; Caner, T. The Direct-Zeff software for direct calculation of mass attenuation coefficient, effective atomic number and effective electron number. *Ann. Nucl. Energy* **2014**, *65*, 158–165. [CrossRef]
27. Chanthima, N.; Kaewkhao, J.; Limkitjaroenporn, P.; Tuscharoen, S.; Kothan, S.; Tungjai, M.; Kaewjaeng, S.; Sarachai, S.; Limsuwan, P. Development of BaO–ZnO–B_2O_3 glasses as a radiation shielding material. *Radiat. Phys. Chem.* **2017**, *137*, 72–77. [CrossRef]
28. Ekinci, N.; Kavaz, E.; Özdemir, Y. A study of the energy absorption and exposure buildup factors of some anti-inflammatory drugs. *Appl. Radiat. Isot.* **2014**, *90*, 265–273. [CrossRef]